OPEN ACCESS

TRANSLATIONAL SCIENCE

Genomic repertoires linked with pathogenic potency of arthritogenic *Prevotella copri* isolated from the gut of patients with rheumatoid arthritis

Takuro Nii,[1,2,3] Yuichi Maeda ,[1,2,4] Daisuke Motooka,[4,5,6] Mariko Naito,[7] Yuki Matsumoto,[6] Takao Ogawa,[1,2] Eri Oguro-Igashira ,[1,2] Toshihiro Kishikawa,[8,9,10] Makoto Yamashita,[11] Satoshi Koizumi,[11] Takashi Kurakawa,[1] Ryu Okumura,[1,4,5] Hisako Kayama,[1,5,12] Mari Murakami,[1,5] Taiki Sakaguchi,[1,5] Bhabatosh Das,[13] Shota Nakamura,[4,5,6,14] Yukinori Okada ,[4,5,8,14,15,16] Atsushi Kumanogoh,[2,4,5,14] Kiyoshi Takeda [1,4,5,14]

Handling editor Josef S Smolen

► Additional supplemental material is published online only. To view, please visit the journal online (http://dx.doi.org/10.1136/ard-2022-222881).

For numbered affiliations see end of article.

Correspondence to
Professor Kiyoshi Takeda, Department of Microbiology and Immunology, Osaka University, Suita 565-0871, Japan; ktakeda@ongene.med.osaka-u.ac.jp

TN and YM are joint first authors.

Received 7 June 2022
Accepted 30 December 2022
Published Online First 10 January 2023

ABSTRACT

Objectives *Prevotella copri* is considered to be a contributing factor in rheumatoid arthritis (RA). However, in some non-Westernised countries, healthy individuals also harbour an abundance of *P. copri* in the intestine. This study investigated the pathogenicity of RA patient-derived *P. copri* (*P. copri*$_{RA}$) compared with healthy control-derived *P. copri* (*P. copri*$_{HC}$).

Methods We obtained 13 *P. copri* strains from the faeces of patients with RA and healthy controls. Following whole genome sequencing, the sequences of *P. copri*$_{RA}$ and *P. copri*$_{HC}$ were compared. To analyse the arthritis-inducing ability of *P. copri*, we examined two arthritis models (1) a collagen-induced arthritis model harbouring *P. copri* under specific-pathogen-free conditions and (2) an SKG mouse arthritis model under *P. copri*-monocolonised conditions. Finally, to evaluate the ability of *P. copri* to activate innate immune cells, we performed in vitro stimulation of bone marrow-derived dendritic cells (BMDCs) by *P. copri*$_{RA}$ and *P. copri*$_{HC}$.

Results Comparative genomic analysis revealed no apparent differences in the core gene contents between *P. copri*$_{RA}$ and *P. copri*$_{HC}$, but pangenome analysis revealed the high genome plasticity of *P. copri*. We identified a *P. copri*$_{RA}$-specific genomic region as a conjugative transposon. In both arthritis models, *P. copri*$_{RA}$-induced more severe arthritis than *P. copri*$_{HC}$. In vitro BMDC stimulation experiments revealed the upregulation of IL-17 and Th17-related cytokines (IL-6, IL-23) by *P. copri*$_{RA}$.

Conclusion Our findings reveal the genetic diversity of *P. copri*, and the genomic signatures associated with strong arthritis-inducing ability of *P. copri*$_{RA}$. Our study contributes towards elucidation of the complex pathogenesis of RA.

WHAT IS ALREADY KNOWN ON THIS TOPIC

⇒ Rheumatoid arthritis (RA) has been associated with a relative expansion of faecal *Prevotella copri*, which is reportedly the dominant bacteria in the gut of healthy individuals with non-Westernised lifestyle.

⇒ *P. copri* exhibits a highly genetic and functional diversity in accordance with host's lifestyle.

WHAT THIS STUDY ADDS

⇒ Comparative genomic analysis revealed that *P. copri* derived from patients with RA (*P. copri*$_{RA}$) possesses a specific genomic region as a conjugative transposon (CTn). These unique genes within CTn were mediated by horizontal gene transfer.

⇒ *P. copri*$_{RA}$ induced more severe arthritis in mouse arthritis models than *P. copri* from healthy controls.

HOW THIS STUDY MIGHT AFFECT RESEARCH, PRACTICE OR POLICY

⇒ The selective elimination of *P. copri*$_{RA}$ may be an effective therapeutic method for patients with RA who harbour *P. copri*$_{RA}$ in their intestine.

INTRODUCTION

Rheumatoid arthritis (RA) is a systemic autoimmune disease that affects multiple joints.[1] Although treatment has rapidly progressed, the aetiology of RA is still not fully understood.[2] Both genetic and environmental factors are thought to contribute to the development of RA.[3] Environmental factors causing RA include smoking, hormonal factors, infection and the composition of the gut microbiota.[4–7] Among these factors, the gut microbiota plays a pivotal role in the development of murine models of arthritis.[8 9] Many studies have demonstrated the altered composition of the intestinal microbiota (dysbiosis) in patients with RA.[10–13] Several studies have shown that some patients with RA harbour an increased proportion of *Prevotella* species, especially *Prevotella copri*, in the intestine.[14–16] Moreover, a recent study showed that *Prevotella* species are dominant in the intestine of some individuals at preclinical stages of RA.[17] Immune responses against *P. copri*-derived antigen are shown to be associated with RA pathogenesis.[18 19] However, in non-Westernised countries, healthy individuals with a plant-rich diet also harbour an abundance of *P. copri* possessing plant polysaccharide-metabolising

To cite: Nii T, Maeda Y, Motooka D, *et al*. *Ann Rheum Dis* 2023;**82**:621–629.

enzymes in the intestine.[20–25] Thus, it is controversial as to whether *P. copri* is harmful or beneficial to the host.

A study involving whole genome sequencing of *P. copri* isolated from the human intestine and large-scale metagenomic sequencing, showed that this bacterium is diverse, consisting of four genetically-distinct clades.[26 27] Genomic variations in *P. copri* have been shown to be linked to the utilisation of polysaccharides.[28] Strain-level diversity of *P. copri* was also investigated by metagenomic shotgun sequencing of the gut microbiota, and differences were shown to be dependent on the host's diet.[29] However, it remained to be determined whether *P. copri* strains present in the intestine of patients with RA were different from those of healthy individuals.

In this study, we isolated *P. copri* strains from patients with RA and healthy individuals from two different geographical regions, and characterised their genomic structures and functional potency, particularly in terms of their pathogenic effects on arthritis.

MATERIALS AND METHODS

Materials and methods are provided in online supplemental information.

RESULTS

Isolation of *P. copri* from patients with RA and healthy controls

To examine whether *P. copri* derived from patients with RA (*P. copri*$_{RA}$) and *P. copri* from healthy controls (*P. copri*$_{HC}$) possess differential effects on arthritis development, we isolated *P. copri* from the faeces of patients with RA and healthy individuals. For this purpose, we recruited 17 patients with RA and 14 healthy controls (cohort 1) who were the participants in the previous study[15] and 55 patients with RA and 28 healthy individuals (cohort 2). There was no apparent difference of dietary habitants between patients with RA and healthy individuals (online supplemental table 1). Among them, faeces of two patients with RA from cohort 1, eight patients with RA and six healthy controls from cohort 2 with the high abundance of *P. copri* were used for isolation of *P. copri* (online supplemental figure 1A,B). It is possible that *P. copri* present in healthy individuals living in different geographical regions has distinct characteristics. Therefore, we also recruited healthy Indians, who showed the high abundance of *P. copri*, and two faeces were used for the isolation.[21] Information on disease condition of the participants was summarised in online supplemental table 2. We successfully obtained 12 isolates from 5 patients with RA (P9, F3, N001, N016, N115), 9 isolates from three healthy Japanese controls (H012, H019, H105) and 7 isolates from two healthy Indian controls (Ind63, Ind117) (online supplemental figure 1C). These isolates were confirmed to be *P. copri* by 16S rRNA gene sequencing.

Differential genomic structures of *P. copri* from patients with RA and healthy controls

To investigate the genetic differences between *P. copri*$_{RA}$ and *P. copri*$_{HC}$, we performed whole genome sequence analysis of 28 isolates of *P. copri* from 5 patients with RA (12 isolates), 5 healthy controls (16 isolates) and the reference strain JCM 13464. Next, we performed average nucleotide identity analysis and defined isolates with >99% similarity as identical (online supplemental table 3). As a result, 28 isolates we obtained and whole genome sequenced were found to be 13 different strains. We isolated five strains (RA-P9, RA-F3, RA-N001, RA-N016, RA-N115) of *P. copri* from patients with RA (*P. copri*$_{RA}$), three strains (HC-H012, HC-H019, HC-H105) of *P. copri* derived from Japanese healthy controls (*P. copri*$_{HC}$) and five strains (HC-Ind63-1, HC-Ind63-2, HC-Ind63-3, HC-Ind117-1, HC-Ind63-2) from Indian healthy controls (online supplemental table 4). The predicted protein coding sequences (CDSs) were obtained in all the isolates by homology based in silico annotation. To define key genomic components, we constructed the pangenome of *P. copri* from 13 strains. This analysis showed that each *P. copri* possessed 2817–3661 genes (online supplemental figure 2A), a core genome of 605 genes and a pangenome consisting of 13 482 genes (online supplemental figure 2B).

Phylogenetic analysis was performed based on 284 conserved genes using genome sequences obtained from 15 strains in a previous study,[26] our 13 strains and the reference strain JCM 13464. Consistent with previous studies,[24 26 28] the 13 *P. copri* strains were genetically categorised into three distinct clades (figure 1A). The majority of the strains (11 out of 13 strains) belonged to clade A. Among the 11 strains belonging to clade A, 4 strains were derived from patients with RA (4 out of 5 strains) and 7 were from healthy controls (7 out of 8 strains). Thus, there were no apparent differences in conserved gene contents between *P. copri*$_{RA}$ and *P. copri*$_{HC}$. These results suggested that the pangenome of *P. copri* could be classified as an open pangenome with high genome plasticity.

We next focused on the species-specific regions. Overviews of genome annotation for the 13 *P. copri* strains revealed that *P. copri*$_{RA}$ possessed a unique genomic region outside of the core region (figure 1B). We then analysed whether this genomic region was present only in microbiota of patients with RA. Using the data of faecal metagenome shotgun sequencing of patients with RA and healthy controls including participants of other previous study (cohort 3),[30] we assessed the number of reads for this genomic region. The relative number of this genomic region in faecal samples from patients with RA was higher than those of healthy controls (figure 1C, online supplemental figure 2C). We further analysed whether this genomic region was present in other bacterial species by performing homology search of this sequence in blastn pipeline. Among registered bacterial strains, only one bacterium, *P. copri* strain YF2 chromosome (Accession number: CP0424641), was found to possess this region. Thus, this genomic region was present only in *P. copri*.

To analyse whether this additive genomic region of *P. copri*$_{RA}$ was associated with the pathogenesis of RA, we analysed protein CDSs in this region by a nucleotide blast search (figure 2). The size of the *P. copri*$_{RA}$-specific region was approximately 100 kilobase pair (kbp) and this region encoded approximately 90 to 100 CDSs. Almost 70% of the CDSs in this region were hypothetical proteins with no characterised function. Genetic plasticity of the bacterial pangenome is triggered by genetic rearrangement including inversions, duplications and horizontal gene transfer (HGT) mediated by a variety of mobile and mobilisable elements such as a conjugative transposon (CTn).[31 32] CTns, which are integrated into the microbial genome, are reported to transfer genes involved in antibiotic resistance,[33–35] the use of alternative carbon sources[36 37] and virulence factors.[38 39] The *P. copri*$_{RA}$-specific region of each strain contained sequences sharing a set of backbone genes for integration-related and conjugal transfer-related functions, which were originally identified in *Porphyromonas*, *Prevotella* and *Bacteroides* species.[40–42] An integrase gene was localised at the start of the *P. copri*$_{RA}$-specific genomic region. In addition, CTn-related genes, such as the cluster of transfer genes including genes encoding DNA primase and mobilisation protein/coupling protein, were observed. Moreover, the

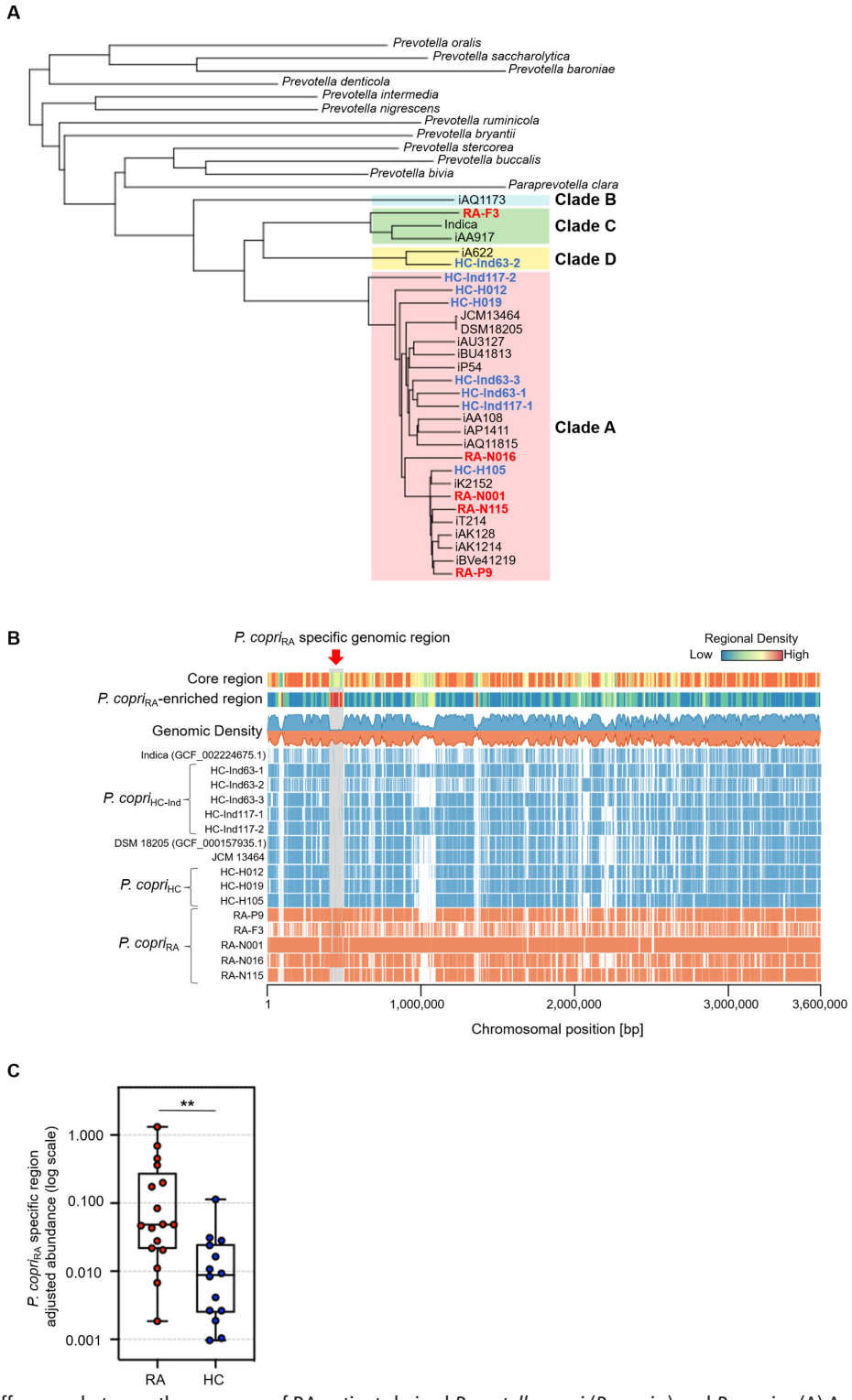

Figure 1 Structural differences between the genomes of RA patient-derived *Prevotella copri* (*P. copri*$_{RA}$) and *P. copri*$_{HC}$. (A) A whole-genome phylogenetic tree analysis revealed that *P. copri* strains, which were isolated in this study, were categorised into three distinct clades. Tree was inferred with FastME 2.1.6.1 from Genome Blast Distance Phylogeny (GBDP) distances calculated from genome sequences. The branch lengths are scaled in terms of GBDP distance formula d5. The numbers above branches are GBDP pseudo-bootstrap support values >60% from 100 replications, with an average branch support of 31.2%. The tree was rooted at the midpoint. (B) Comparison of the genomic regions between *P. copri*$_{RA}$ and *P. copri*$_{HC}$ strains. The presence of each genomic region is represented by colour at the chromosomal position, using strain N001-13 as reference. *P. copri*$_{RA}$ and *P. copri*$_{HC}$ strains are coloured red and blue, respectively. *P. copri*$_{RA}$ and *P. copri*$_{HC}$ core regions of density are shown by genomic density of a filled-line plot. The *P. copri*$_{RA}$-specific genomic region is indicated by a grey background. (C) Comparison of the abundance of the *P. copri*$_{RA}$-specific genomic region in faecal DNA between patients with RA and HC from cohorts 1, 2 and 3. Seventeen patients with RA (cohort 1: n=2, cohort 2: n=10, cohort 3: n=5) and 14 HC (cohort 1: n=1, cohort 2: n=6, cohort 3: n=7) of which the relative abundance of *P. copri* was higher than 1% were selected for analysis. Box and whisker plots show median, 25th and 75th percentiles, and minimum and maximum values. Two-tailed Mann-Whitney U test was performed for statistical analysis. **p<0.01. HC, healthy controls; RA, rheumatoid arthritis.

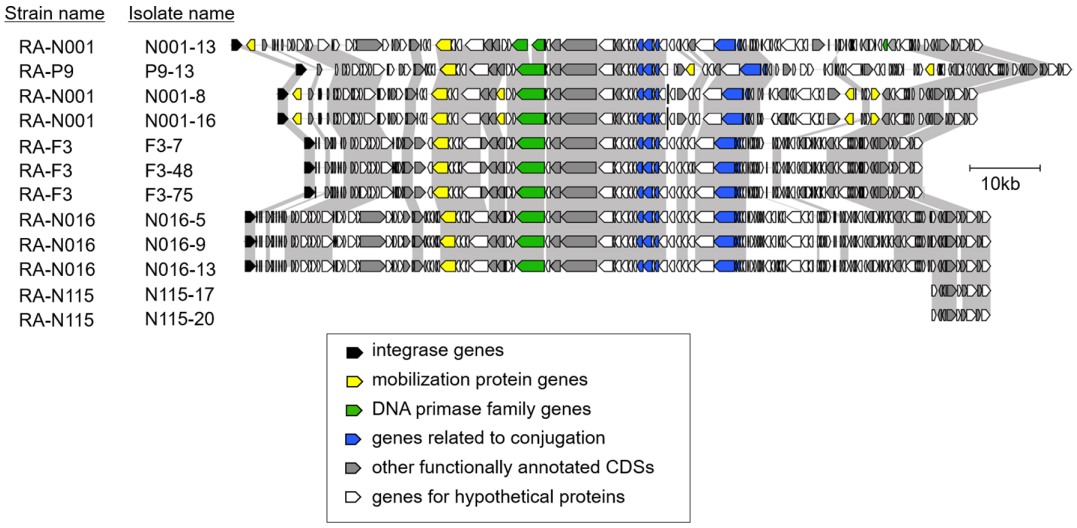

Figure 2 Conjugative transposon (CTn) identified in the RA patient-derived *Prevotella copri* (*P. copri*$_{RA}$)-specific region. The gene organisations of CTns identified in the *P. copri*$_{RA}$-specific regions are shown. The coding sequences (CDSs) are depicted by arrows (black arrow, integrase genes; yellow arrow, mobilisation protein; green arrow, DNA primase family protein; blue arrow, genes related to conjugation; grey arrow, other functionally annotated CDSs; and white arrow, genes for hypothetical proteins). The grey shading indicates homologous CDSs with >70% amino acid sequence identity. RA, rheumatoid arthritis.

sequences of these genes in this specific genome region were highly conserved among *P. copri*$_{RA}$ strains. These results indicated that the *P. copri*$_{RA}$-specific region was a CTn, which we named CTnPc, on the pangenome of *P. copri*$_{RA}$. To examine the insertion site for CTnPc, we analysed the region adjacent to CTnPc on the genome. In strains from the same patient, CTn was present at the same position on the genome. However, the insertion site was different for each patient, with the exception of patients P9 and N001. These results suggested that CTnPc was inserted into different sites on the genome of each strain driven by HGT events.

Development of severe collagen-induced arthritis in mice harbouring *P. copri*$_{RA}$

We next analysed the arthritis-inducing ability of *P. copri*$_{RA}$ and *P. copri*$_{HC}$ using mouse models. We orally administered 6.0×10^{10} of *P. copri*$_{RA}$ (RA-N001) and *P. copri*$_{HC}$ (HC-H012) to DBA/1 J mice reared under specific-pathogen-free (SPF) conditions; however, both *P. copri*$_{RA}$ and *P. copri*$_{HC}$ failed to colonise the intestine of SPF mice (online supplemental figure 3A,B). Therefore, in a subsequent experiment, SPF-DBA/1J mice were first orally treated with combinations of antibiotics (ampicillin, neomycin, metronidazole and vancomycin) for 5 days to reduce the intestinal microbiota, and then orally inoculated with 6.0×10^{10} of *P. copri*$_{RA}$ (RA-N001) or *P. copri*$_{HC}$ (HC-H012) for five consecutive days (online supplemental figure 3C). Under these conditions, both *P. copri*$_{RA}$ (RA-N001) and *P. copri*$_{HC}$ (HC-H012) successfully colonised the intestines to a similar extent (online supplemental figure 3D). Using these DBA/1J mice harbouring *P. copri*$_{RA}$ (RA-N001) or *P. copri*$_{HC}$ (HC-H012), we induced collagen-induced arthritis by challenging on two occasions (days 0 and 21) with type II collagen (online supplemental figure 3E). On day 21, at the time point of the second challenge, monitoring of the arthritis score and the incidence of arthritis was initiated. DBA/1J mice harbouring *P. copri*$_{RA}$ (RA-N001) developed more severe arthritis, as evidenced by a higher arthritis score (figure 3A) and an earlier onset and higher incidence of arthritis (figure 3B), compared with mice harbouring *P. copri*$_{HC}$ (HC-H012). More serious arthritis development in DBA/1J mice harbouring *P. copri*$_{RA}$ (RA-N001) was confirmed by more severe swelling of ankle joints (figure 3C) and more severe histological changes in ankle joints, such as proliferation of synovial lining cells, infiltration of inflammatory cells and bone destruction associated with pannus formation (figure 3D,E). Moreover, the serum concentration of type II collagen-specific IgG at day 63 was higher in DBA/1J mice harbouring *P. copri*$_{RA}$ (RA-N001) than in mice harbouring *P. copri*$_{HC}$ (HC-H012) (figure 3F). The more severe arthritis observed in DBA/1J mice harbouring *P. copri*$_{RA}$ (RA-N001) was not due to the preservation of a higher number of *P. copri*$_{RA}$ (RA-N001) in the intestine because there were almost equal proportions and numbers of *P. copri*$_{RA}$ (RA-N001) and *P. copri*$_{HC}$ (HC-H012) in the intestines of DBA/1J mice during the course of the experiments (online supplemental figure 4A–C).

Because effector T helper (Th) cells, particularly Th1 and Th17 cells, have been shown to be involved in the pathogenesis of collagen-induced arthritis,[9 43 44] we next analysed the number of Th1 and Th17 cells in popliteal lymph nodes (PLN). At 77 days after the first immunisation, cells were isolated from PLNs, stimulated with phorbol 12-myristate 13-acetate and ionomycin, and analysed the production of IFN-γ and IL-17A from $CD4^+$ T cells by flow cytometry. Although the proportion of Th1 and Th17 cells remained unaltered, the number of Th1 and Th17 cells was increased in DBA/1J mice harbouring *P. copri*$_{RA}$ compared with mice harbouring *P. copri*$_{HC}$ (figure 3G,H).

We then analysed whether other *P. copri*$_{RA}$ strains possess the arthritis-inducing ability and CTnPc is implicated in the pathogenesis. For this purpose, each of *P. copri*$_{RA}$ strains with CTnPc (RA-P9, RA-N001, RA-N016: RA+), a *P. copri*$_{RA}$ strain without CTnPc (RA-N115: RA−), *P. copri*$_{HC}$ strains (HC-H012, HC-H019, HC-H105: HC) was colonised in the intestine of DBA/1J mice (online supplemental figure 5A). For control, DBA/1J mice with oral administration of phosphate buffered saline (PBS) was also prepared. Severities of collagen-induced arthritis in DBA/1J mice harbouring a *P. copri*$_{RA}$ strain without CTnPc (RA-N115) or *P. copri*$_{HC}$ strains (HC-H012, HC-H019, or HC-H105) were similar to those with DBA/1J mice with PBS. In contrast, DBA/1J mice harbouring *P. copri*$_{RA}$ strains

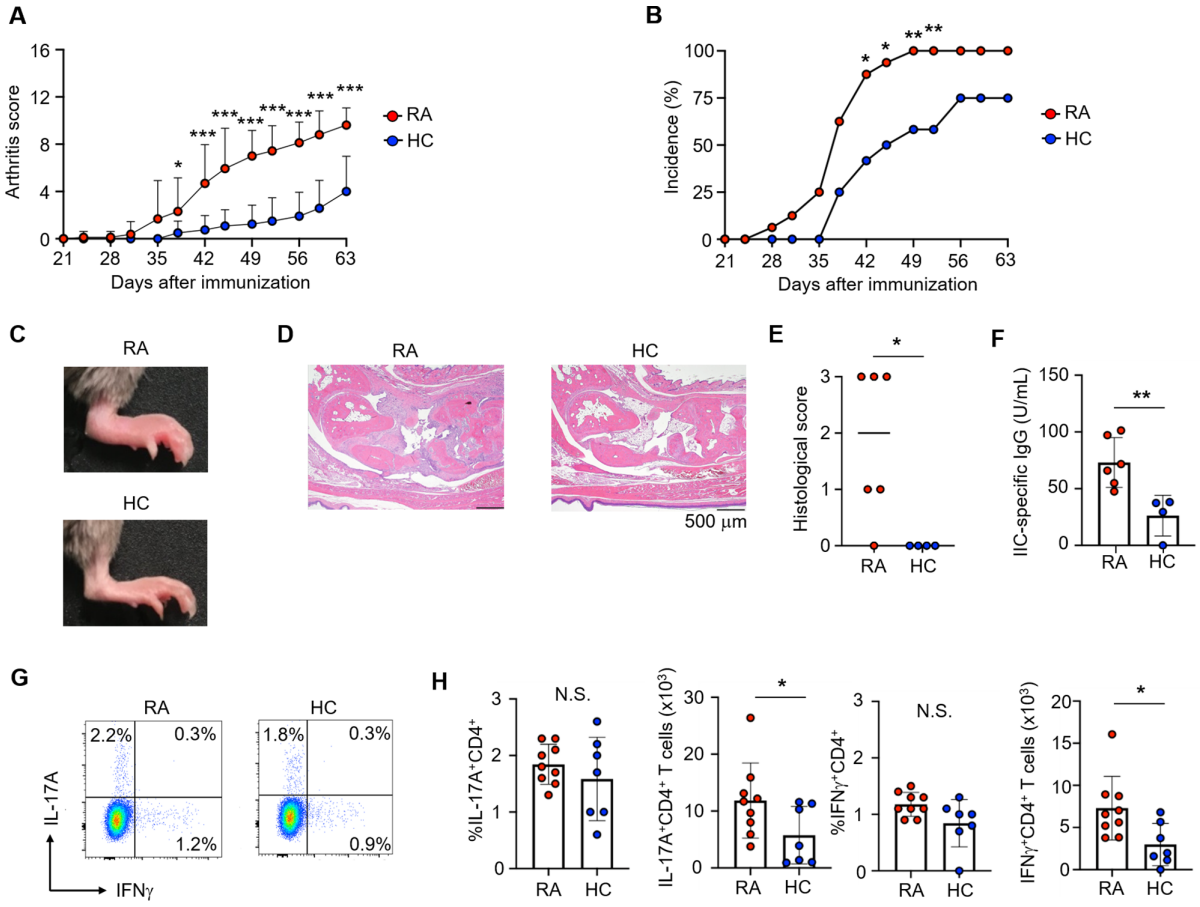

Figure 3 Severe collagen-induced arthritis in RA patient-derived *Prevotella copri* (*P. copri*$_{RA}$)-colonised DBA/1 J mice (A, B) Arthritis scores (A) and incidence (B) of *P. copri*-inoculated DBA/1 J mice in collagen-induced arthritis (CIA) models under specific-pathogen-free (SPF) conditions. Data are pooled from two independent experiments and total numbers of mice are as follows: *P. copri*$_{RA}$ (RA-N001 strain)-inoculated mice (RA), n=16; *P. copri*$_{HC}$ (HC-H012)-inoculated mice (HC), n=12. Each symbol and vertical line represents the mean±SD. (C) Photographic images of the ankle joint of *P. copri*-inoculated mice at day 63 after primary immunisation with type II collagen. (D, E) Histopathology (D) and histological score (E) of the lower ankle joint at day 63 after primary immunisation (RA; n=6, HC; n=4). One representative histological image is shown. H&E staining. (F) The concentration of type II collagen-specific IgG in sera at day 63 after primary immunisation was determined by ELISA (RA; n=6 and HC; n=4). Bar graphs show data as the mean±SD. (G) Representative flow cytometry plots of popliteal lymph node (PLN) cells of RA or HC in CIA models under SPF conditions. (H) Percentage and number of IL17A$^+$ CD4$^+$ cells and IFNγ$^+$ CD4$^+$ cells in PLN cells. These cells were analysed by flow cytometry after stimulation with phorbol myristate acetate (PMA) and ionomycin at day 77 after primary immunisation (RA; n=9 and HC; n=7). Bar graphs show data as the mean±SD. One-way ANOVA followed by a Tukey's multiple comparisons test (A), χ^2-test (B), and two-tailed Mann-Whitney U tests (E, F, H) were performed for statistical analyses. *p<0.05, **p<0.01, ***p<0.001, N.S., not significant. (E–H) Data were reproduced in three independent experiments with similar results. ANOVA, analysis of variance; HC, healthy controls; RA, rheumatoid arthritis.

with CTnPc (RA-P9, RA-N001, or RA-N016) developed severe arthritis, as evidenced by higher arthritis score and incidence (online supplemental figure 5B,C). We analysed the proportion and number of immune cell subsets including CD19$^+$ B cells, CD4$^+$ and CD8$^+$ T cells in spleen (online supplemental figure 5D,E) and mesenteric lymph node (online supplemental figure 5F,G), CD11b$^+$CD11c$^+$, CD11b$^+$CD11c$^-$, and CD11b$^-$CD11c$^+$ myeloid cells in lamina propria of large intestine (online supplemental figure 5H,I) in addition to Th1 and Th17 CD4$^+$ T cells in PLN (online supplemental figure 5J,K). Although the proportion of all of these immune cells were similar among all the mice, the number of only Th17 cells in PLN was increased in DBA/1J mice harbouring *P. copri*$_{RA}$ strains with CTnPc (RA-P9, RA-N001, or RA-N016) (online supplemental figure 5K). Taken together, these results suggested that the colonisation of *P. copri*$_{RA}$ in the intestines induced severe inflammation in a collagen-induced arthritis model with slight increases in the Th1 and Th17 responses.

Development of severe arthritis in SKG mice harbouring *P. copri*$_{RA}$

We next analysed whether *P. copri*$_{RA}$ alone can induce severe arthritis. We orally inoculated germ-free SKG mice with 1.0×10^8*P. copri*$_{RA}$ (RA-N001) and *P. copri*$_{HC}$ (HC-H012) once (online supplemental figure 6A). Both *P. copri*$_{RA}$ (RA-N001) and *P. copri*$_{HC}$ (HC-H012) similarly colonised the intestines of SKG mice, as evidenced by the similar number of *P. copri* detected in the faeces by quantitative (Q)-PCR (online supplemental figure 6B). We also performed fluorescence in situ hybridisation of the large intestine of SKG mice inoculated with *P. copri*$_{RA}$ (RA-N001) and *P. copri*$_{HC}$ (HC-H012) using a bacteria-specific probe (online supplemental figure 6C). Both *P. copri*$_{RA}$ (RA-N001) and *P. copri*$_{HC}$ (HC-H012) were found to be present in the lumen of the large intestine.

Then, SKG mice monocolonised with *P. copri*$_{RA}$ (RA-N001) or *P. copri*$_{HC}$ (HC-H012) were injected with zymosan to induce

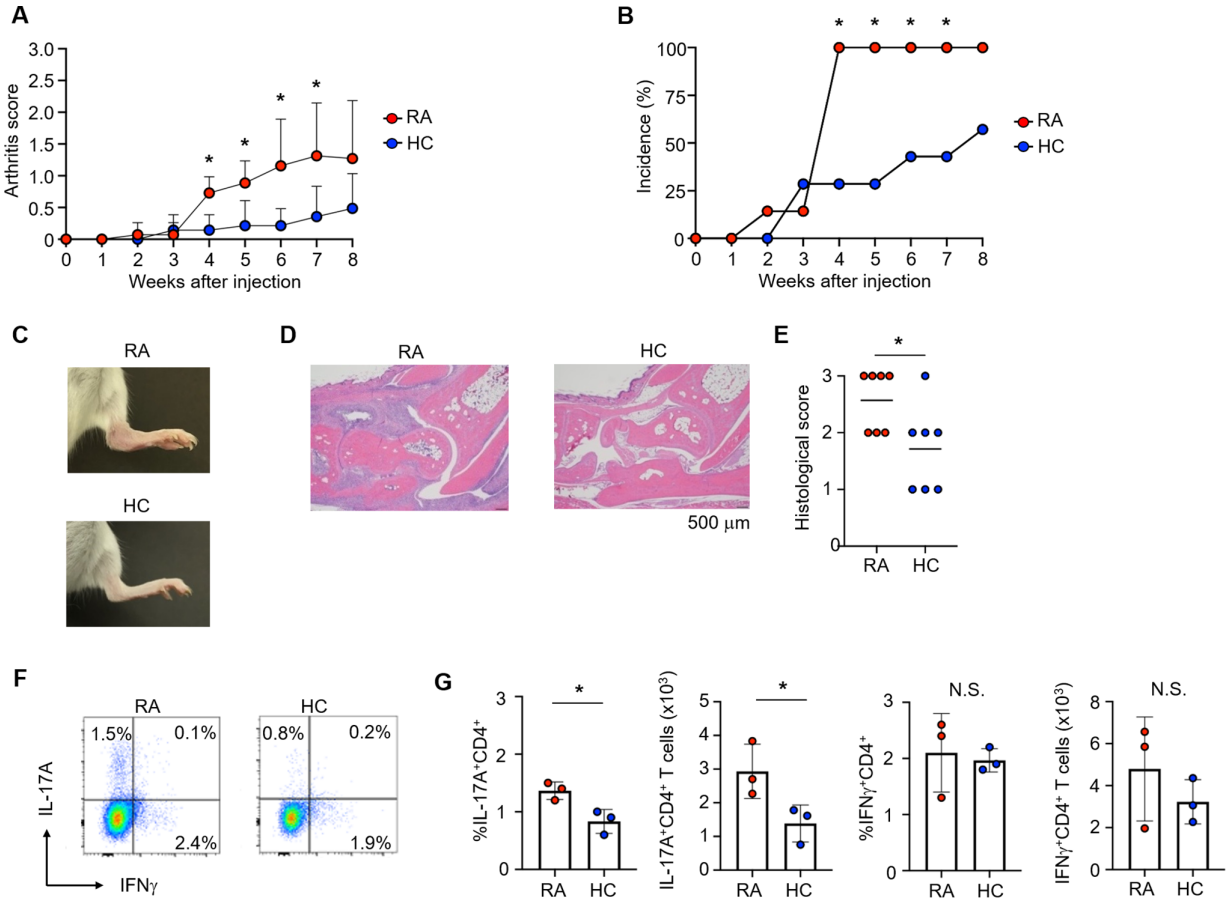

Figure 4 Severe arthritis in RA patient-derived *Prevotella copri* (*P. copri*$_{RA}$)-monocolonised SKG mice. (A, B) Arthritis score (A) and incidence (B) of *P. copri*-monocolonised SKG mice after the injection of zymosan (RA-N001-monocolonised (RA); n=7, HC-H012-monocolonised (HC); n=7). Each symbol and vertical line represents the mean±SD. (C) Photographic images of the ankle joint of *P. copri*-monocolonised mice at day 56 after the injection of zymosan. (D, E) Histopathology (D) and histological score (E) of the lower ankle joint at day 56 after the injection of zymosan (RA; n=7, HC; n=7). One representative histological image is shown. H&E staining. (F) Representative flow cytometry plots of PLN cells of RA-N001 or HC-H012-monocolonised mice in the SKG arthritis model. (G) Percentage and number of IL17A$^+$ CD4$^+$ cells and IFNγ$^+$ CD4$^+$ cells in PLN cells. These cells were analysed by flow cytometry after stimulation with phorbol myristate acetate (PMA) and ionomycin at day 56 after the injection of zymosan (RA; n=3 and HC; n=3). Bar graphs show data as the mean±SD. Two-tailed Student's t-test (A, E, G) and χ^2-test (B) were performed for statistical analysis. *p<0.05. N.S.=not significant. All data were reproduced in another independent experiment with similar results. HC, healthy controls; RA, rheumatoid arthritis.

arthritis (online supplemental figure 6D).[45] SKG mice monocolonised with *P. copri*$_{RA}$ (RA-N001) developed more severe arthritis after zymosan treatment compared with SKG mice monocolonised with *P. copri*$_{HC}$ (HC-H012), as shown by the higher arthritis score (figure 4A) as well as the higher incidence of arthritis (figure 4B). The more severe development of arthritis in SKG mice monocolonised with *P. copri*$_{RA}$ (RA-N001) was affirmed by the more severe swelling of ankle joints (figure 4C) and the more severe synovial inflammation and bone destruction in the ankle joints (figure 4D,E). These results suggested that *P. copri*$_{RA}$ has strong arthritis-inducing ability.

Aberrant Th17 responses of autoimmune T cells are implicated in the development of arthritis in SKG mice.[46 47] Therefore, the number of Th1 and Th17 cells in PLNs was analysed in SKG mice monocolonised with *P. copri*$_{RA}$ (RA-N001) and *P. copri*$_{HC}$ (HC-H012). The proportion and number of Th17 cells was increased in SKG mice monocolonised with *P. copri*$_{RA}$ (RA-N001) compared with those monocolonised with *P. copri*$_{HC}$ (HC-H012) (figure 4F,G). Taken together, these findings may indicate that the colonisation of *P. copri*$_{RA}$ in the intestines induced severe arthritis via the activation of Th17 cells in SKG mice.

P. copri$_{RA}$-mediated activation of innate immune cells

Based on these findings, we hypothesised that *P. copri*$_{RA}$ is a potent inducer of Th17 cells that induce inflammation in the joints, and analysed the mechanisms by which Th17 cells were induced in *P. copri*$_{RA}$-colonised mice. There is a previous report demonstrating that the heat-stable components of *P. copri* activate innate immune cells (antigen-presenting cells) and increase expression of major histocompatibility complex (MHC) class II and production of Th17-related cytokines such as IL-6 and IL-23.[15] Although there were no differences in the proportion or number of CD11b$^+$CD11c$^+$, CD11b$^+$CD11c$^-$, CD11b$^-$CD11c$^+$ cells in the large intestine (online supplemental figure 5J), the intensity of MHC class II expression in the intestinal CD11b$^+$CD11c$^+$ cells was upregulated in DBA/1J mice harbouring *P. copri*$_{RA}$ with CTnPc (RA-P9, RA-N001, or RA-N016) compared with mice harbouring *P. copri*$_{RA}$ without CTnPc (RA-N115) or *P. copri*$_{HC}$ strains (HC-H012, HC-H019, or HC-H105) (online supplemental figure 7A). These results suggest that intestinal colonisation with *P. copri*$_{RA}$ resulted in activation of innate immune cells in the intestinal lamina propria.

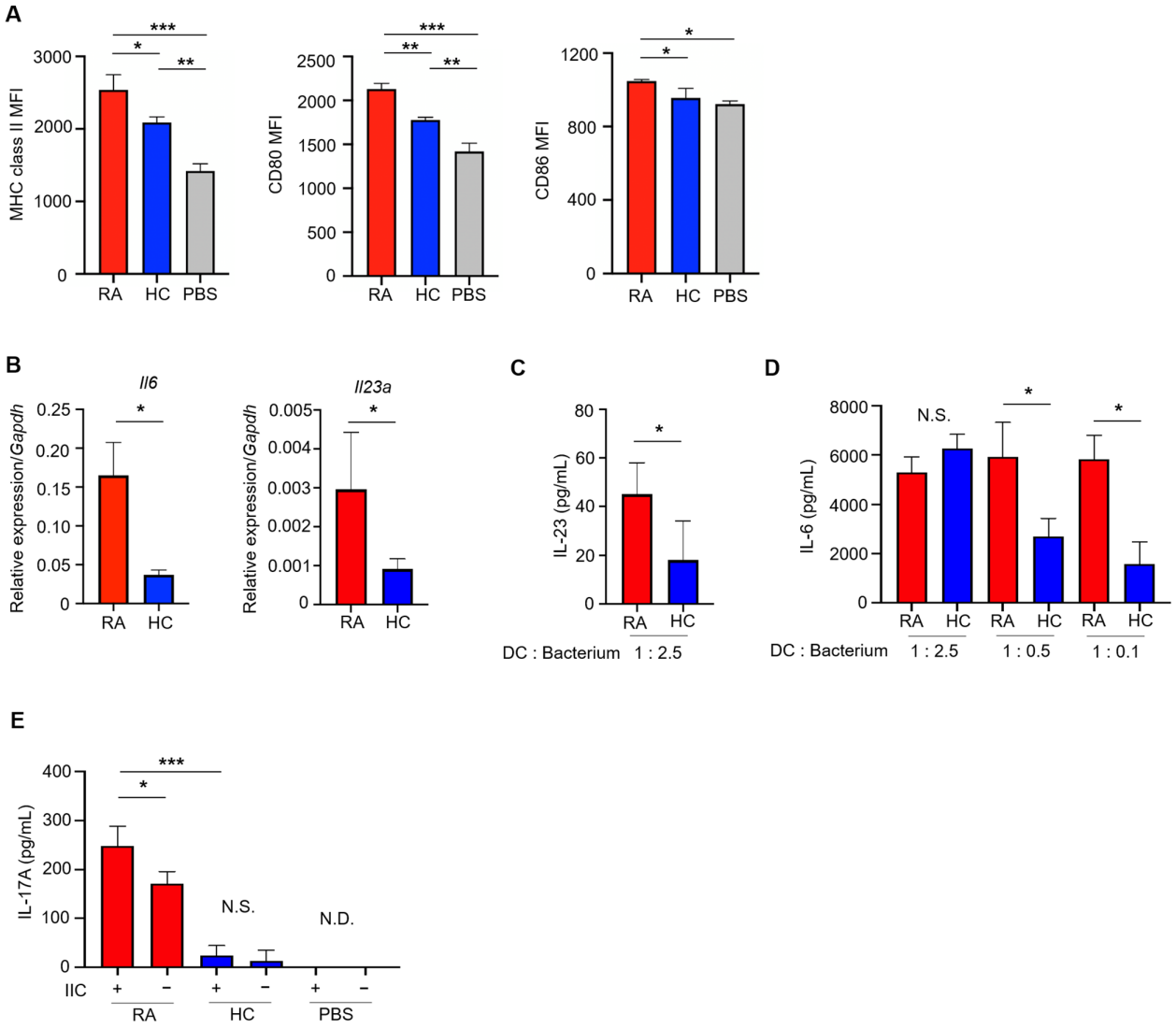

Figure 5 Activation of T cells by RA patient-derived Prevotella copri (*P. copri*$_{RA}$)-treated dendritic cells. (A) Expression levels of major histocompatibility complex (MHC) class II, CD80 and CD86 molecules in bone marrow-derived dendritic cells (BMDCs) stimulated with heat-killed *P. copri*$_{RA}$ (RA-N001: RA) or *P. copri*$_{HC}$ (HC-H012: HC) or PBS for 72 hours. Expression of MHC class II, CD80 and CD86 in the BMDCs was determined as the mean fluorescence intensity (MFI) by flow cytometric analysis. (B) Q-PCR analysis of *Il6* and *Il23a* mRNA expression in BMDCs stimulated with heat-killed *P. copri*$_{RA}$ (RA-N001: RA) or *P. copri*$_{HC}$ (HC-H012: HC). (C, D) Concentrations of IL-23 (C) and IL-6 (D) were measured by ELISA in the supernatants of BMDCs stimulated with the indicated heat-killed *P. copri*$_{RA}$ (RA-N001: RA) or *P. copri*$_{HC}$ (HC-H012: HC). (E) The concentration of IL-17A was measured by ELISA in the supernatants of naïve CD4$^+$ cells co-cultured with BMDCs stimulated by *P. copri*$_{RA}$ (RA-N001: RA) or *P. copri*$_{HC}$ (HC-H012: HC). Cells were stimulated with or without bovine type II collagen (IIC). Bar graphs show data as the mean±SD. of triplicate measurements. One-way ANOVA followed by a Tukey's multiple comparison tests (A, E) and two-tailed Mann-Whitney U tests (B–D) were performed for statistical analyses. *p<0.05, **p<0.01, ***p<0.001, N.S.=not significant. N.D.=not detected. All data are representative of at least three independent experiments. ANOVA, analysis of variance; HC, healthy controls; RA, rheumatoid arthritis.

To determine whether *P. copri*$_{RA}$ is more effective at activating innate immune cells, we performed in vitro experiments using bone marrow-derived dendritic cells (BMDCs). BMDCs were stimulated with heat-killed *P. copri*$_{RA}$ (RA-N001) or *P. copri*$_{HC}$ (HC-H012) and analysed for the expression of MHC class II, CD86 and CD80 (figure 5A). Compared with *P. copri*$_{HC}$, *P. copri*$_{RA}$ induced higher expression of MHC class II, CD86 and CD80, as evidenced by a higher mean fluorescence intensity. We also analysed the expression of mRNA of Th17-related cytokine genes, *Il6* and *Il23a*, in BMDCs stimulated with *P. copri*$_{RA}$ or *P. copri*$_{HC}$ by Q-PCR (figure 5B). *P. copri*$_{RA}$ induced higher expression of both genes than *P. copri*$_{HC}$. The production of IL-6 and IL-23 proteins from *P. copri*$_{RA}$-stimulated BMDCs was also analysed by ELISA (figure 5C,D). IL-23 production was higher in *P. copri*$_{RA}$-stimulated BMDCs (DC: *P. copri* ratio=1: 2.5) than in *P. copri*$_{HC}$-stimulated BMDCs. IL-6 production was similar in BMDCs stimulated with *P. copri*$_{RA}$ and *P. copri*$_{HC}$ (DC: *P. copri* ratio=1: 2.5). However, when the number of *P. copri* used for stimulation was reduced, IL-6-inducing capacity was sustained in *P. copri*$_{RA}$, but not in *P. copri*$_{HC}$. We next examined whether *P. copri*$_{RA}$ possesses a higher ability to induce antigen-specific Th17 cells from naïve CD4$^+$ T cells. BMDCs of DBA/1J mice were first treated with *P. copri*$_{RA}$ or *P. copri*$_{HC}$. Then, naïve CD4$^+$ T cells from DBA/1J mice were co-cultured with the *P. copri*-treated dendritic cells (DC: *P. copri* ratio=1: 2.5) for 5 days. Type II collagen was then added and cells were co-cultured for an additional 2 days. After a total of 7 days of co-culturing with BMDCs, T cells were stimulated with type II collagen and analysed for

the production of IL-17A (figure 5E). T cells co-cultured with *P. copri*$_{RA}$-stimulated BMDCs produced higher amounts of IL-17A. We also analysed the responses to other strains: *P. copri*$_{RA}$ with CTnPc (RA-P9, or RA-N016: RA+), *P. copri*$_{RA}$ without CTnPc (RA-N115: RA−) or *P. copri*$_{HC}$ (HC-H019, or HC-H105: HC). BMDCs stimulated with *P. copri*$_{RA}$ with CTnPc expressed the higher level of MHC class II (online supplemental figure 7B) and produced higher amounts of IL-6, IL-23 and TNF-a (online supplemental figure 7C) compared with those stimulated with *P. copri*$_{RA}$ without CTnPc or *P. copri*$_{HC}$. Induction of T cell IL-17 response was induced potently by stimulation with *P. copri*$_{RA}$ with CTnPc (online supplemental figure 7D). These results indicated that *P. copri*$_{RA}$ strongly induced a Th17 response via the activation of dendritic cells.

DISCUSSION

In this study, we isolated *P. copri* strains from the faeces of patients with RA (*P. copri*$_{RA}$) and healthy individuals (*P. copri*$_{HC}$), and found that *P. copri*$_{RA}$ strains possess a unique region in their genome. Furthermore, colonisation of *P. copri*$_{RA}$ in mouse intestines caused severe pathologies in two different mouse arthritis models.

RA is an immune disorder caused by the complex interaction of genetic and environmental factors.[3] Considering environmental factors, mucosal surfaces are potentially an important site for triggering RA development.[3] Indeed, smoking, which affects the airway mucosa, is a prominent environmental factor contributing to the development of RA.[48] Periodontitis, mainly caused by *Porphyromonas gingivalis* in the oral mucosa, is also implicated in RA pathogenesis.[49] Furthermore, many studies in recent years have shown that dysbiosis in the intestinal mucosa is associated with susceptibility to RA.[10–13] Among studies focusing on dysbiosis of the intestinal microbiota, *Prevotella* species, particularly *P. copri*, are often increased in patients with RA.[14–17] However, *P. copri* is also predominant among the intestinal microbiota of healthy individuals with a diet rich in plant-derived fibre.[20–25] Based on the findings of this study, we propose that colonisation of pathogenic *P. copri*, rather than *Prevotella*-predominant dysbiosis, in the intestines is one of the causes of RA pathogenesis.

We found that *P. copri*$_{RA}$ possesses a distinct genomic structure from that of *P. copri*$_{HC}$. *P. copri* is genetically highly diverse and can be classified into at least four different clades.[26 27] Among these clades, *P. copri* strains belonging to clade A are the most abundant.[24 26] Many of the *P. copri* strains isolated in this study also belonged to clade A, including both *P. copri*$_{RA}$ and *P. copri*$_{HC}$ strains. This indicated that the different genomic structures between *P. copri*$_{RA}$ and *P. copri*$_{HC}$ strains did not result from distinct clades. However, we found that unique sequences were conserved among *P. copri*$_{RA}$ strains and contained CDSs characteristic to CTn-related genes that mediate HGT. Thus, *P. copri*$_{RA}$ is thought to have acquired a unique genome (CTnPc) by HGT.

A recent study isolated the antigen, Pc-p27, from *P. copri* from a patient with RA who was presented on HLA-DR and a triggered immune response.[18 19] The Pc-p27 gene exists in four out of five *P. copri*$_{RA}$ strains and six out of eight *P. copri*$_{HC}$ strains. Thus, the Pc-p27 gene is not selectively present in *P. copri*$_{RA}$ (online supplemental table 5) and therefore does not correlate with the pathogenicity of *P. copri*$_{RA}$. *P. copri*$_{RA}$ was more potent than *P. copri*$_{HC}$ in activating innate immune cells, as evidenced by the enhanced surface expression of MHC class II and the increased cytokine production from mouse myeloid cells. Thus, the pathogenicity of *P. copri*$_{RA}$ might correlate with the capacity to induce a strong innate immune response. By activating innate immune cells and thereby enhancing Pc-p27 antigen presentation by MHC class II, *P. copri*$_{RA}$ may induce more severe arthritis.

Within the *P. copri*$_{RA}$-specific genome region (CTnPc), many genes encoding hypothetical proteins reside (online supplemental table 6). Genes present in the CTnPc region are expected to exert pathogenic ability to activate innate immunity, ultimately leading to the development of arthritis. To identify a pathogenic factor in the CTnPc region of *P. copri*$_{RA}$, we attempted to generate mutant *P. copri*$_{RA}$ strains. However, we encountered difficulty in introducing gene modifications into *P. copri*. Recently, a novel gene tool to introduce gene insertions and deletions into *P. copri* has been developed,[24] which may aid identification of the pathogenic factor responsible for arthritis development in a future study.

In this study, we successfully isolated pathogenic strains of *P. copri* from the faeces of patients with RA. Development of a system to detect *P. copri*$_{RA}$ would be a good strategy to predict the future development of RA. In addition, the development of a method to selectively eliminate *P. copri*$_{RA}$ may be an effective therapeutic measure for patients with RA who harbour *P. copri*$_{RA}$ in their intestine.

Author affiliations
[1]Laboratory of Immune Regulation, Department of Microbiology and Immunology, Graduate School of Medicine, Osaka University, Osaka, Japan
[2]Department of Respiratory Medicine, Clinical Immunology, Graduate School of Medicine, Osaka University, Osaka, Japan
[3]National Hospital Organization Osaka Toneyama Medical Center, Osaka, Japan
[4]Integrated Frontier Research for Medical Science Division, Institute for Open and Transdisciplinary Research Initiatives, Osaka University, Osaka, Japan
[5]WPI Immunology Frontier Research Center, Osaka University, Osaka, Japan
[6]Department of Infection Metagenomics, Research Institute for Microbial Diseases, Osaka University, Osaka, Japan
[7]Department of Microbiology and Oral Infection, Graduate School of Biomedical Sciences, Nagasaki University, Nagasaki, Japan
[8]Department of Statistical Genetics, Graduate School of Medicine, Osaka University, Osaka, Japan
[9]Department of Otorhinolaryngology-Head and Neck Surgery, Graduate School of Medicine, Osaka University, Osaka, Japan
[10]Department of Head and Neck Surgery, Aichi Cancer Center Hospital, Aichi, Japan
[11]Research & Innovation Center, Kyowa Hakko Bio Co., Ltd, Ibaraki, Japan
[12]Institute for Advanced Co-Creation Studies, Osaka University, Osaka, Japan
[13]Molecular Genetics Laboratory, Infection and Immunology Division, Translational Health Science and Technology Institute, Faridabad, India
[14]Center for Infectious Disease Education and Research, Osaka University, Osaka, Japan
[15]Department of Genome Informatics, Graduate School of Medicine, the University of Tokyo, Tokyo, Japan
[16]Laboratory for Systems Genetics, RIKEN Center for Integrative Medical Sciences, Kanagawa, Japan

Acknowledgements We thank Y. Magota for technical assistance, Kate Fox from Edanz (https://jp.edanz.com/ac) for editing a draft of this manuscript, and C. Hidaka for secretarial assistance.

Contributors TN performed the experiments, analysed the data and wrote the manuscript; YMae performed the experiments and analyzed the data; DM, MN, YMat, TO, EO-I, TKi, MY, SK, TKu, RO, HK, MM and TS assisted with experiments; BD, SN, YO and AK supervised the study; KT planned and directed the overall project and wrote the manuscript and is the guarantor.

Funding This study was supported by grants from the Ministry of Education, Culture, Sports, Science and Technology of Japan (JP18H04028 and JP20K20595) and the Japan Agency for Medical Research and Development (JP20gm1010004h0005).

Competing interests None declared.

Patient and public involvement Patients and/or the public were not involved in the design, or conduct, or reporting, or dissemination plans of this research.

Patient consent for publication Not applicable.

Ethics approval This study was approved by the ethical committee of Osaka University. Participants gave informed consent to participate in the study before taking part.

Provenance and peer review Not commissioned; externally peer reviewed.

Data availability statement Data are available on reasonable request.

ORCID iDs
Yuichi Maeda http://orcid.org/0000-0002-6831-8205
Eri Oguro-Igashira http://orcid.org/0000-0001-5863-0775
Yukinori Okada http://orcid.org/0000-0002-0311-8472
Kiyoshi Takeda http://orcid.org/0000-0002-1778-6332

REFERENCES

1 Scott DL, Wolfe F, Huizinga TWJ. Rheumatoid arthritis. *Lancet* 2010;376:1094–108.
2 Narazaki M, Tanaka T, Kishimoto T. The role and therapeutic targeting of IL-6 in rheumatoid arthritis. *Expert Rev Clin Immunol* 2017;13:535–51.
3 Firestein GS, McInnes IB. Immunopathogenesis of rheumatoid arthritis. *Immunity* 2017;46:183–96.
4 Konig MF, Abusleme L, Reinholdt J, *et al*. Aggregatibacter actinomycetemcomitans-induced hypercitrullination links periodontal infection to autoimmunity in rheumatoid arthritis. *Sci Transl Med* 2016;8:369ra176.
5 Alpízar-Rodríguez D, Finckh A. Environmental factors and hormones in the development of rheumatoid arthritis. *Semin Immunopathol* 2017;39:461–8.
6 Balandraud N, Roudier J. Epstein-Barr virus and rheumatoid arthritis. *Joint Bone Spine* 2018;85:165–70.
7 Nii T, Kuzuya K, Kabata D, *et al*. Crosstalk between tumor necrosis factor-alpha signaling and aryl hydrocarbon receptor signaling in nuclear factor -kappa B activation: a possible molecular mechanism underlying the reduced efficacy of TNF-inhibitors in rheumatoid arthritis by smoking. *J Autoimmun* 2019;98:95–102.
8 Wu H-J, Ivanov II, Darce J, *et al*. Gut-residing segmented filamentous bacteria drive autoimmune arthritis via T helper 17 cells. *Immunity* 2010;32:815–27.
9 Evans-Marin H, Rogier R, Koralov SB, *et al*. Microbiota-Dependent involvement of Th17 cells in murine models of inflammatory arthritis. *Arthritis Rheumatol* 2018;70:1971–83.
10 Zhang X, Zhang D, Jia H, *et al*. The oral and gut microbiomes are perturbed in rheumatoid arthritis and partly normalized after treatment. *Nat Med* 2015;21:895–905.
11 Vaahtovuo J, Munukka E, Korkeamäki M, *et al*. Fecal microbiota in early rheumatoid arthritis. *J Rheumatol* 2008;35:1500–5.
12 Chen J, Wright K, Davis JM, *et al*. An expansion of rare lineage intestinal microbes characterizes rheumatoid arthritis. *Genome Med* 2016;8:43.
13 Picchianti-Diamanti A, Panebianco C, Salemi S, *et al*. Analysis of gut microbiota in rheumatoid arthritis patients: disease-related dysbiosis and modifications induced by etanercept. *Int J Mol Sci* 2018;19. doi:10.3390/ijms19102938. [Epub ahead of print: 27 Sep 2018].
14 Scher JU, Sczesnak A, Longman RS, *et al*. Expansion of intestinal Prevotella copri correlates with enhanced susceptibility to arthritis. *Elife* 2013;2:e01202.
15 Maeda Y, Kurakawa T, Umemoto E, *et al*. Dysbiosis contributes to arthritis development via activation of autoreactive T cells in the intestine. *Arthritis Rheumatol* 2016;68:2646–61.
16 Lee J-Y, Mannaa M, Kim Y, *et al*. Comparative analysis of fecal microbiota composition between rheumatoid arthritis and osteoarthritis patients. *Genes* 2019;10. doi:10.3390/genes10100748. [Epub ahead of print: 25 Sep 2019].
17 Alpizar-Rodriguez D, Lesker TR, Gronow A, *et al*. *Prevotella copri* in individuals at risk for rheumatoid arthritis. *Ann Rheum Dis* 2019;78:590–3.
18 Pianta A, Arvikar S, Strle K, *et al*. Evidence of the immune relevance of Prevotella copri, a gut microbe, in patients with rheumatoid arthritis. *Arthritis Rheumatol* 2017;69:964–75.
19 Pianta A, Chiumento G, Ramsden K, *et al*. Identification of novel, immunogenic HLA-DR-Presented Prevotella copri peptides in patients with rheumatoid arthritis. *Arthritis Rheumatol* 2021;73:2200–5.
20 De Filippo C, Cavalieri D, Di Paola M, *et al*. Impact of diet in shaping gut microbiota revealed by a comparative study in children from Europe and rural Africa. *Proc Natl Acad Sci U S A* 2010;107:14691–6.
21 Pareek S, Kurakawa T, Das B, *et al*. Comparison of Japanese and Indian intestinal microbiota shows diet-dependent interaction between bacteria and fungi. *NPJ Biofilms Microbiomes* 2019;5:37.
22 Prasoodanan P K V, Sharma AK, Mahajan S, *et al*. Western and non-Western gut microbiomes reveal new roles of Prevotella in carbohydrate metabolism and mouth-gut axis. *NPJ Biofilms Microbiomes* 2021;7:77.
23 Asnicar F, Berry SE, Valdes AM, *et al*. Microbiome connections with host metabolism and habitual diet from 1,098 deeply phenotyped individuals. *Nat Med* 2021;27:321–32.
24 Li J, Gálvez EJC, Amend L, *et al*. A versatile genetic toolbox for Prevotella copri enables studying polysaccharide utilization systems. *Embo J* 2021;40:e108287.
25 Gálvez EJC, Iljazovic A, Amend L, *et al*. Distinct polysaccharide utilization determines interspecies competition between intestinal Prevotella spp. *Cell Host Microbe* 2020;28:838–52.
26 Tett A, Huang KD, Asnicar F, *et al*. The Prevotella copri complex comprises four distinct clades underrepresented in Westernized populations. *Cell Host Microbe* 2019;26:666–79.
27 Tett A, Pasolli E, Masetti G, *et al*. Prevotella diversity, niches and interactions with the human host. *Nat Rev Microbiol* 2021;19:585–99.
28 Fehlner-Peach H, Magnabosco C, Raghavan V, *et al*. Distinct polysaccharide utilization profiles of human intestinal Prevotella copri isolates. *Cell Host Microbe* 2019;26:680–90.
29 De Filippis F, Pasolli E, Tett A, *et al*. Distinct genetic and functional traits of human intestinal Prevotella copri strains are associated with different habitual diets. *Cell Host Microbe* 2019;25:444–53.
30 Tomofuji Y, Kishikawa T, Maeda Y, *et al*. Whole gut virome analysis of 476 Japanese revealed a link between phage and autoimmune disease. *Ann Rheum Dis* 2022;81:278–88.
31 Wozniak RAF, Waldor MK. Integrative and conjugative elements: mosaic mobile genetic elements enabling dynamic lateral gene flow. *Nat Rev Microbiol* 2010;8:552–63.
32 Johnson CM, Grossman AD. Integrative and conjugative elements (ICEs): what they do and how they work. *Annu Rev Genet* 2015;49:577–601.
33 Mays TD, Smith CJ, Welch RA, *et al*. Novel antibiotic resistance transfer in Bacteroides. *Antimicrob Agents Chemother* 1982;21:110–8.
34 Smith CJ, Markowitz SM, Macrina FL. Transferable tetracycline resistance in Clostridium difficile. *Antimicrob Agents Chemother* 1981;19:997–1003.
35 Rashtchian A, Dubes GR, Booth SJ. Tetracycline-Inducible transfer of tetracycline resistance in Bacteroides fragilis in the absence of detectable plasmid DNA. *J Bacteriol* 1982;150:141–7.
36 Hochhut B, Jahreis K, Lengeler JW, *et al*. CTnscr94, a conjugative transposon found in enterobacteria. *J Bacteriol* 1997;179:2097–102.
37 Rauch PJ, De Vos WM. Characterization of the novel nisin-sucrose conjugative transposon Tn5276 and its insertion in Lactococcus lactis. *J Bacteriol* 1992;174:1280–7.
38 He J, Baldini RL, Déziel E, *et al*. The broad host range pathogen Pseudomonas aeruginosa strain PA14 carries two pathogenicity islands harboring plant and animal virulence genes. *Proc Natl Acad Sci U S A* 2004;101:2530–5.
39 Carter MQ, Chen J, Lory S. The Pseudomonas aeruginosa pathogenicity island PAPI-1 is transferred via a novel type IV pilus. *J Bacteriol* 2010;192:3249–58.
40 Bacic M, Parker AC, Stagg J, *et al*. Genetic and structural analysis of the Bacteroides conjugative transposon CTn341. *J Bacteriol* 2005;187:2858–69.
41 Bonheyo G, Graham D, Shoemaker NB, *et al*. Transfer region of a Bacteroides conjugative transposon, CTnDOT. *Plasmid* 2001;45:41–51.
42 Naito M, Sato K, Shoji M, *et al*. Characterization of the Porphyromonas gingivalis conjugative transposon CTnPg1: determination of the integration site and the genes essential for conjugal transfer. *Microbiology* 2011;157:2022–32.
43 Murphy CA, Langrish CL, Chen Y, *et al*. Divergent pro- and antiinflammatory roles for IL-23 and IL-12 in joint autoimmune inflammation. *J Exp Med* 2003;198:1951–7.
44 Nakae S, Saijo S, Horai R, *et al*. IL-17 production from activated T cells is required for the spontaneous development of destructive arthritis in mice deficient in IL-1 receptor antagonist. *Proc Natl Acad Sci U S A* 2003;100:5986–90.
45 Yoshitomi H, Sakaguchi N, Kobayashi K, *et al*. A role for fungal {beta}-glucans and their receptor Dectin-1 in the induction of autoimmune arthritis in genetically susceptible mice. *J Exp Med* 2005;201:949–60.
46 Hashimoto M, Hirota K, Yoshitomi H, *et al*. Complement drives Th17 cell differentiation and triggers autoimmune arthritis. *J Exp Med* 2010;207:1135–43.
47 Ito Y, Hashimoto M, Hirota K, *et al*. Detection of T cell responses to a ubiquitous cellular protein in autoimmune disease. *Science* 2014;346:363–8.
48 Källberg H, Ding B, Padyukov L, *et al*. Smoking is a major preventable risk factor for rheumatoid arthritis: estimations of risks after various exposures to cigarette smoke. *Ann Rheum Dis* 2011;70:508–11.
49 Lundberg K, Wegner N, Yucel-Lindberg T, *et al*. Periodontitis in RA-the citrullinated enolase connection. *Nat Rev Rheumatol* 2010;6:727–30.